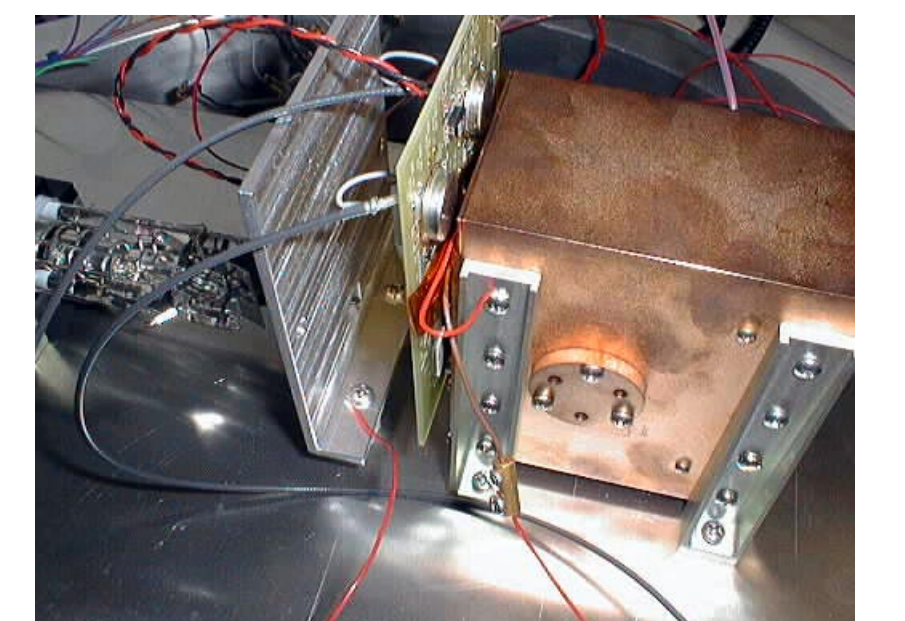# Tomographic Imaging of Electron Distributions

Michael R. Collier, Dennis J. Chornay, Michael Coplan, Norman J. Dionne,
Federico Herrero, Jeff Houser, Michael A. Johnson, John W. Keller,
Paul Rozmarynowski and James A. Slavin

1. Introduction

We describe the development of a new type of electron spectrometer which obtains the electron velocity distribution in a space plasma using a two-dimensional tomographic method. The spectrometer consists of a constant magnetic field cavity with a single entrance aperture and a one dimensional position sensitive microchannel plate/anode assembly for electron detection. Electrons entering through the aperture are deflected by the magnetic field and land on the channel plate assembly at a position dependent on their incident energy and direction. Considering the velocity components v_x in the aperture plane and v_y perpendicular to the aperture plane (see Figure 1), electrons with the same v_y component always land at the same position, independent of the v_x com-

Figure 1.

ponent. This is an exact analytic result and means that the flux of electrons registered at one position on the channel plate assembly represents an integral of the velocity distribution over the v_x component of velocity. A set of anode fluxes represents a set of slices across the velocity distribution function for a given spectrometer orientation in space. As the spectrometer rotates (with the spacecraft), another set of slices is obtained across velocity space. Thus, the collection of slices or tomograms obtained may be inverted with known tomographic techniques (e.g. Radon transform in two dimensions) to obtain the actual velocity distribution function.

2. Motivation

The advantages of this design over previous techniques used to measure electron distributions include: (1) simplicity — the instrument eliminates hardware complexity by relying on mathematical techniques to deconvolve the data (2) passivity — there are no stepping voltages or look angles (3) inexpensive and robust — the simple design makes this instrument an ideal candidate for multi-spacecraft missions and (4) versatility - the deconvolution technique employed may be tailored to fit the end: simple methods for browse or kp data and much more sophisticated methods for specific event data.

This instrument, first proposed by Zhang et al. [Zhang, Y., M.A. Coplan, J.H. Moore and C.A. Berenstein, Computerized tomographic imaging for space plasma physics, J. Appl. Phys., 68, 5883-5889, 1990] takes natural advantage of economic trends which show hardware costs increasing and computational costs decreasing over time (see Figure 2) by simplifying the instrument hardware requirements and instead relying on computationally intensive deconvolution techniques to process the raw data.
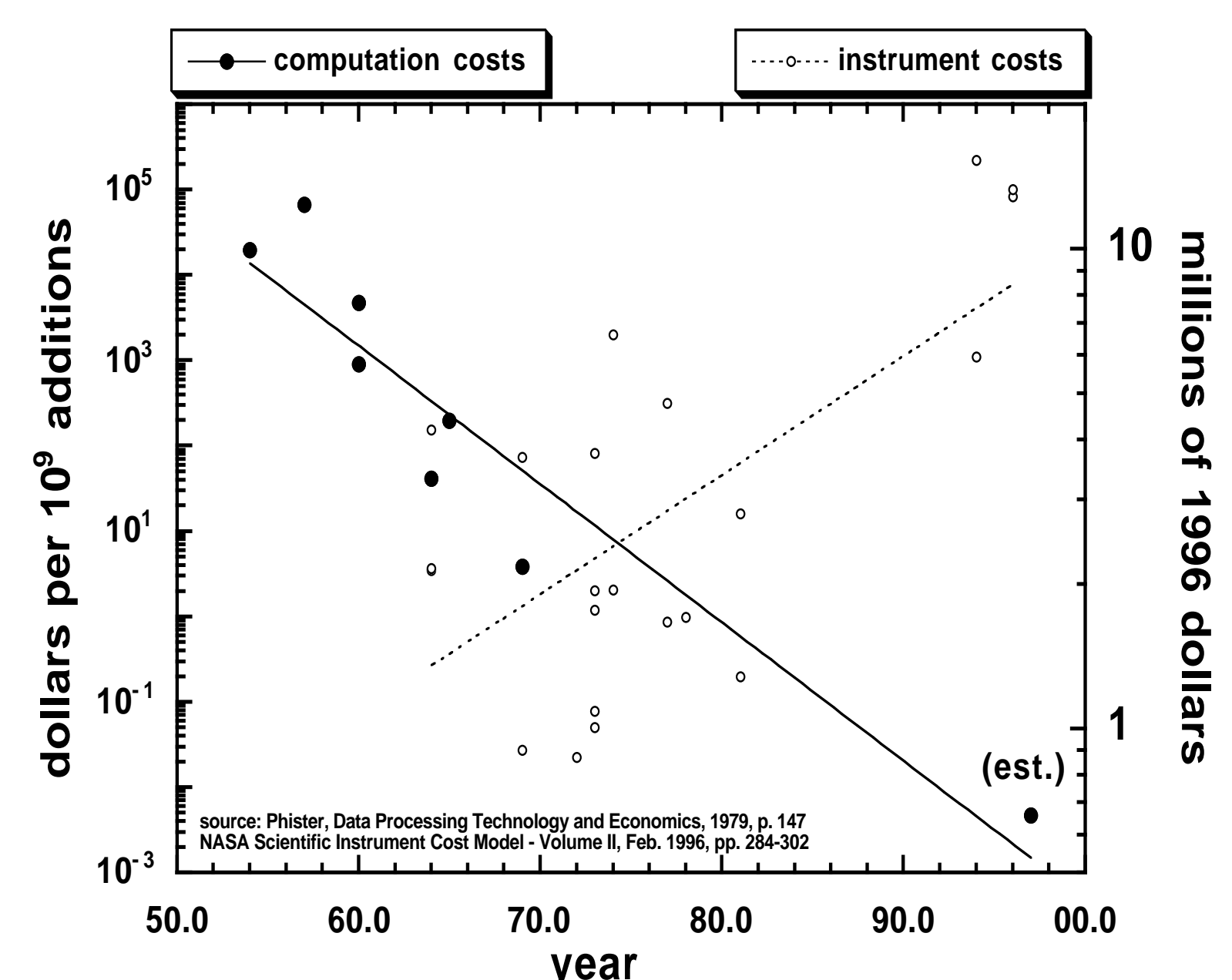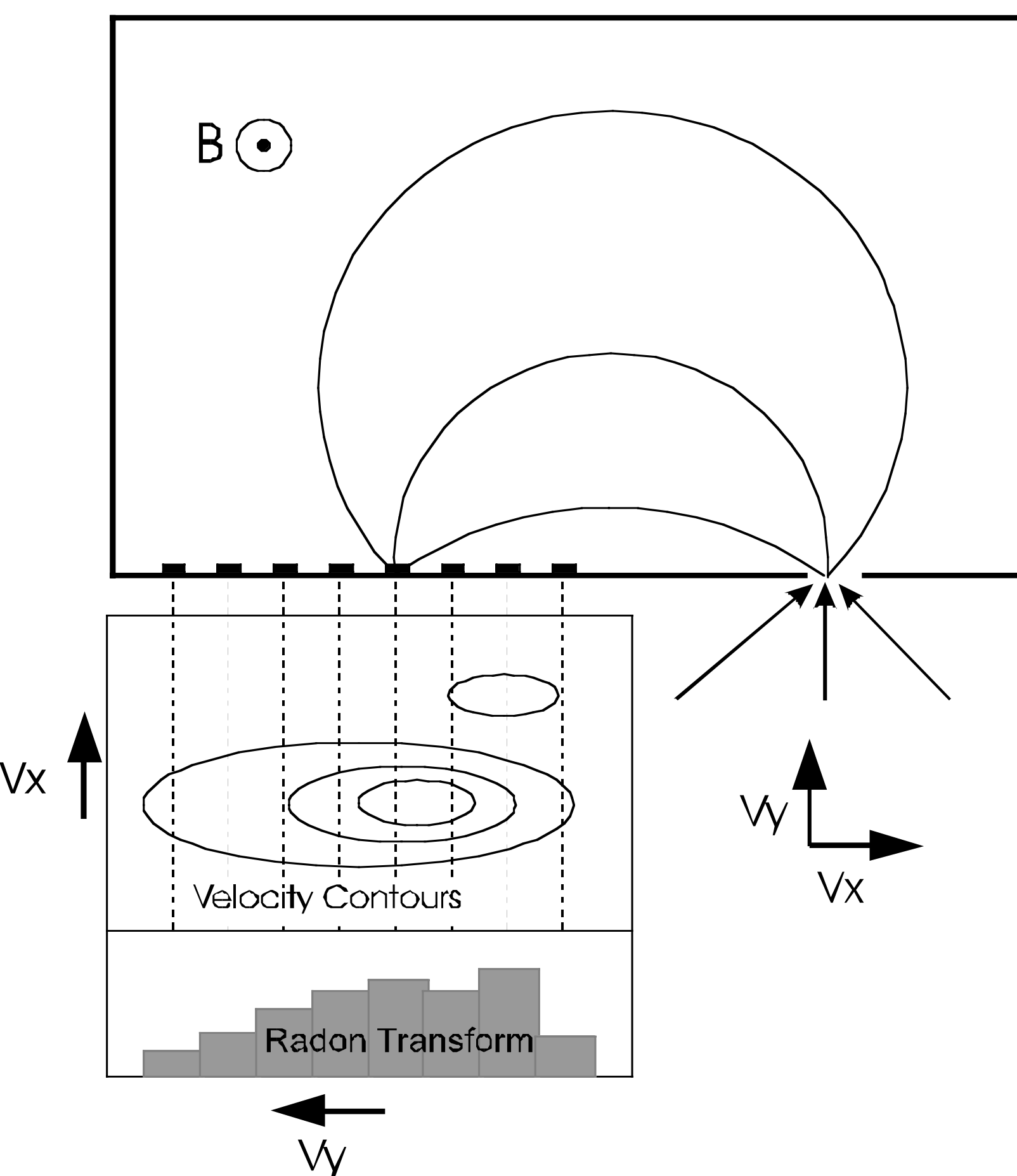

Figure 2.

3. Modelling and Design

The first step in designing the prototype was performing realistic particle simulation for various instrument configurations. The example below, Figure 3, shows sample electron trajectories through a realistic field geometry with an aperture, housing, and microchannel stack.

Based on realistic magnetic field simulations of the region between the pole faces, as shown in Figure 4, it was apparent that to effect a reasonably step-like transition between the field-free region and the region between the pole faces, it would be necessary to have the pole faces at most about 3 mm apart. This is the distance opted for in the prototype design.
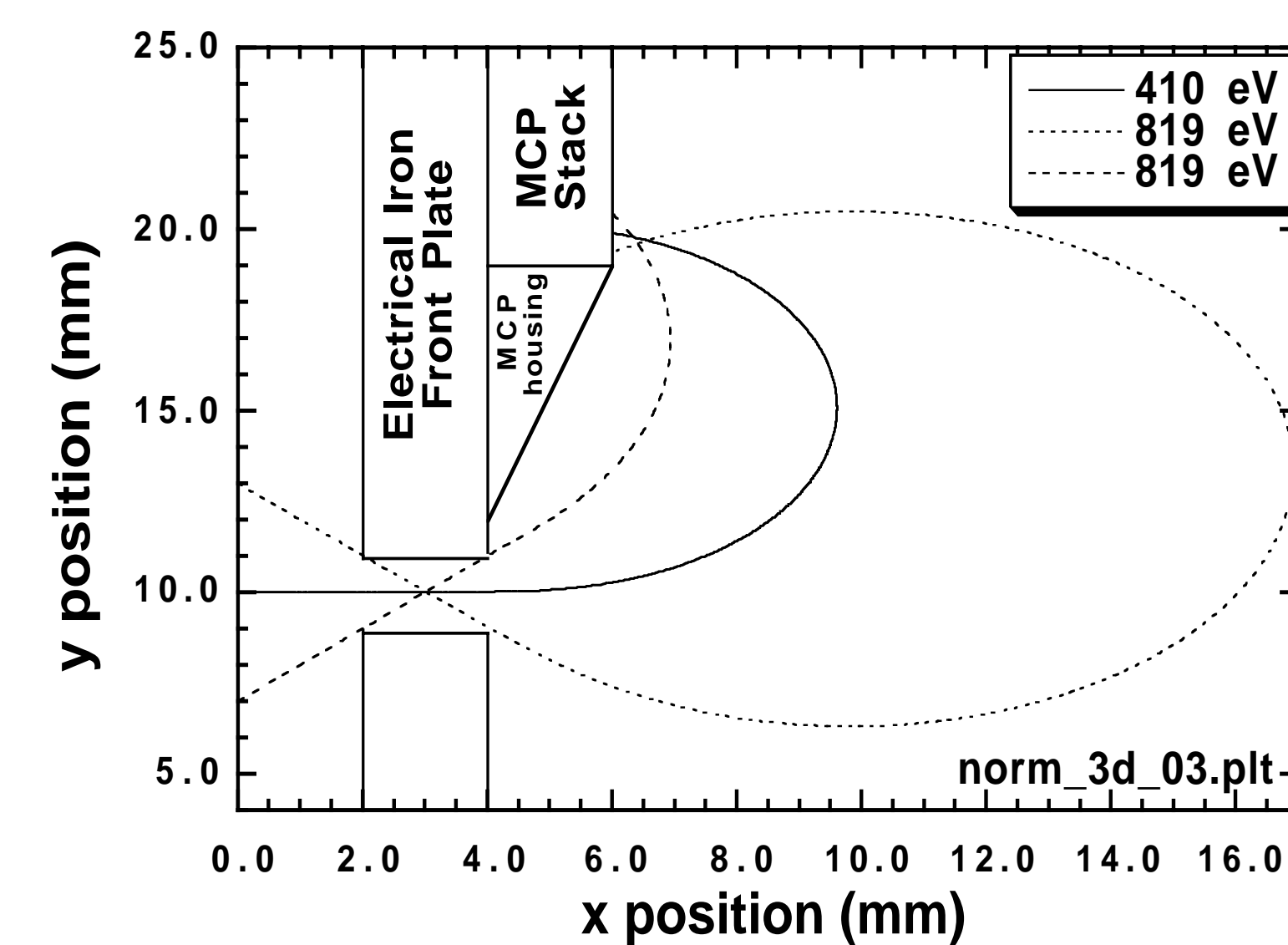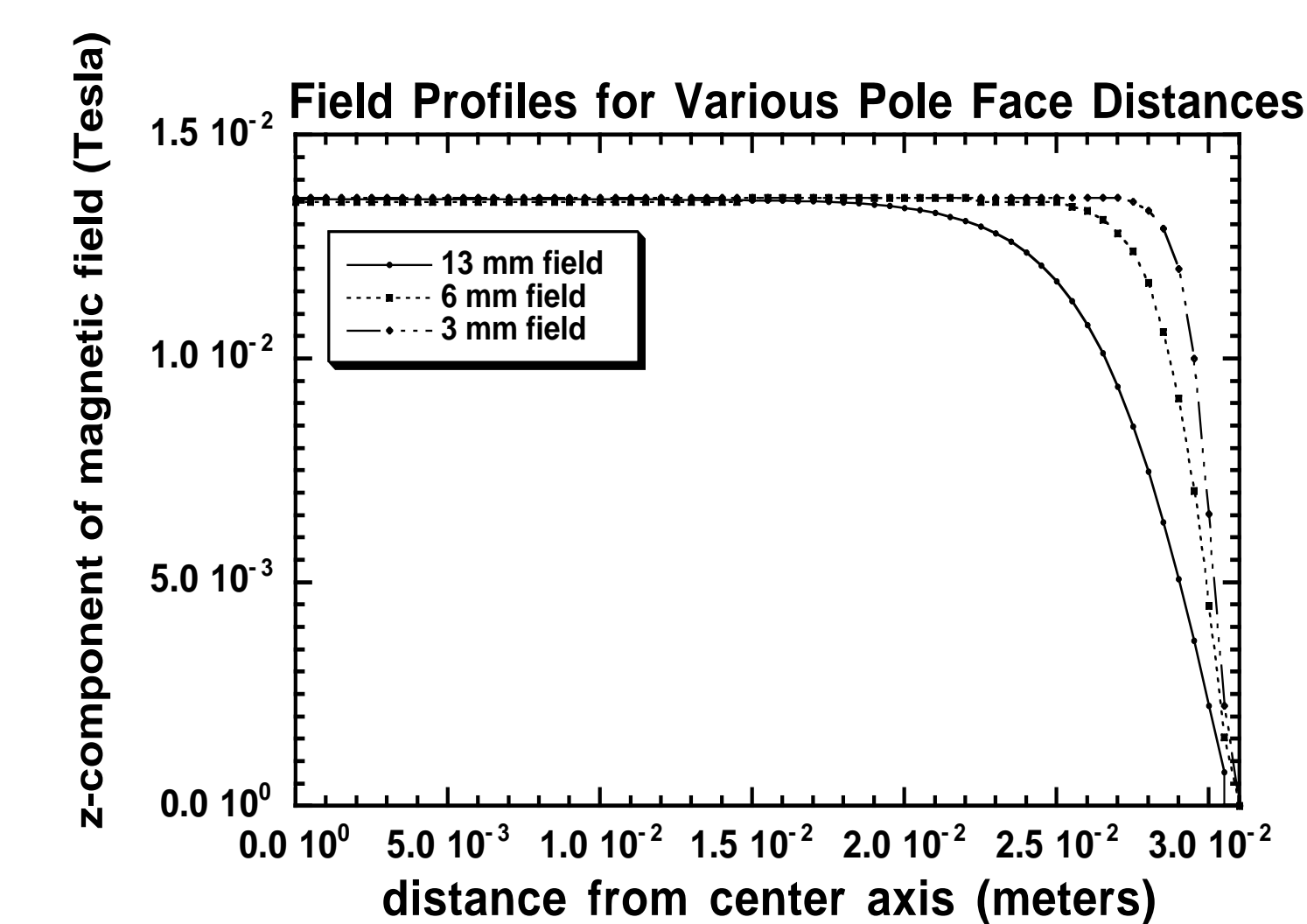

Figure 3.

Figure 4.

Rough fabrication drawings were created based on the simulation results. One of these is shown in Figure 5 below. The pole faces were designed 60 millimeters square with alignment/containment rings (shown here on the inside of the instrument, but eventually placed on the outside) used to hold the cylindrical flux guides. The magnetic field is adjustable, using magnet wedges represented by the orange. The yellow are non-magnetic 70-30 cupro-nickel alignment posts and E-clamps.
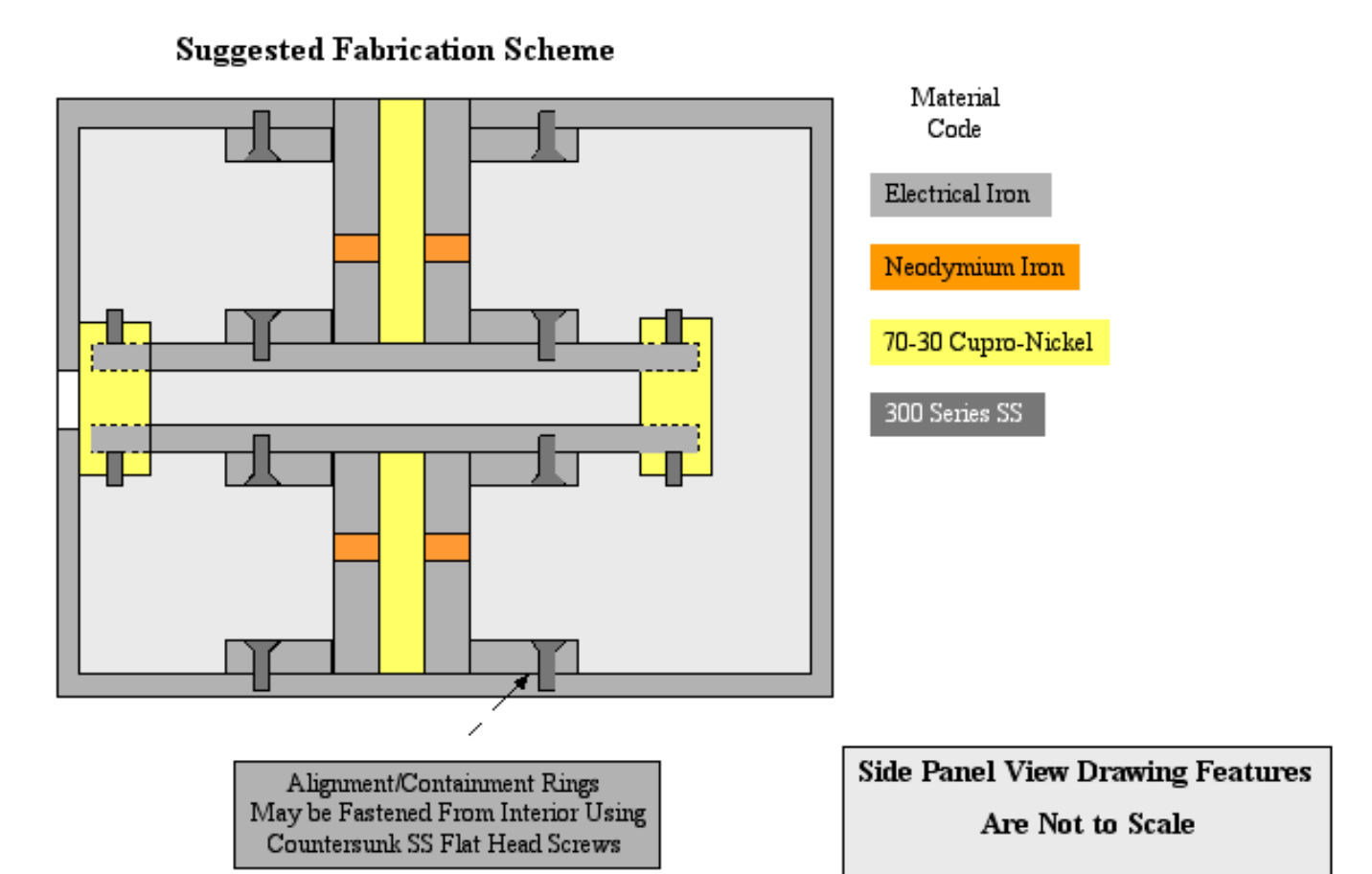

Figure 5.

The pole faces were maintained a fixed three millimeters apart by using four non-magnetic precision E-shaped pole corner separator clamps.

Finally, these sketches were turned into actual mechanical drawings. One of the isometric drawing is shown as Figure 6.
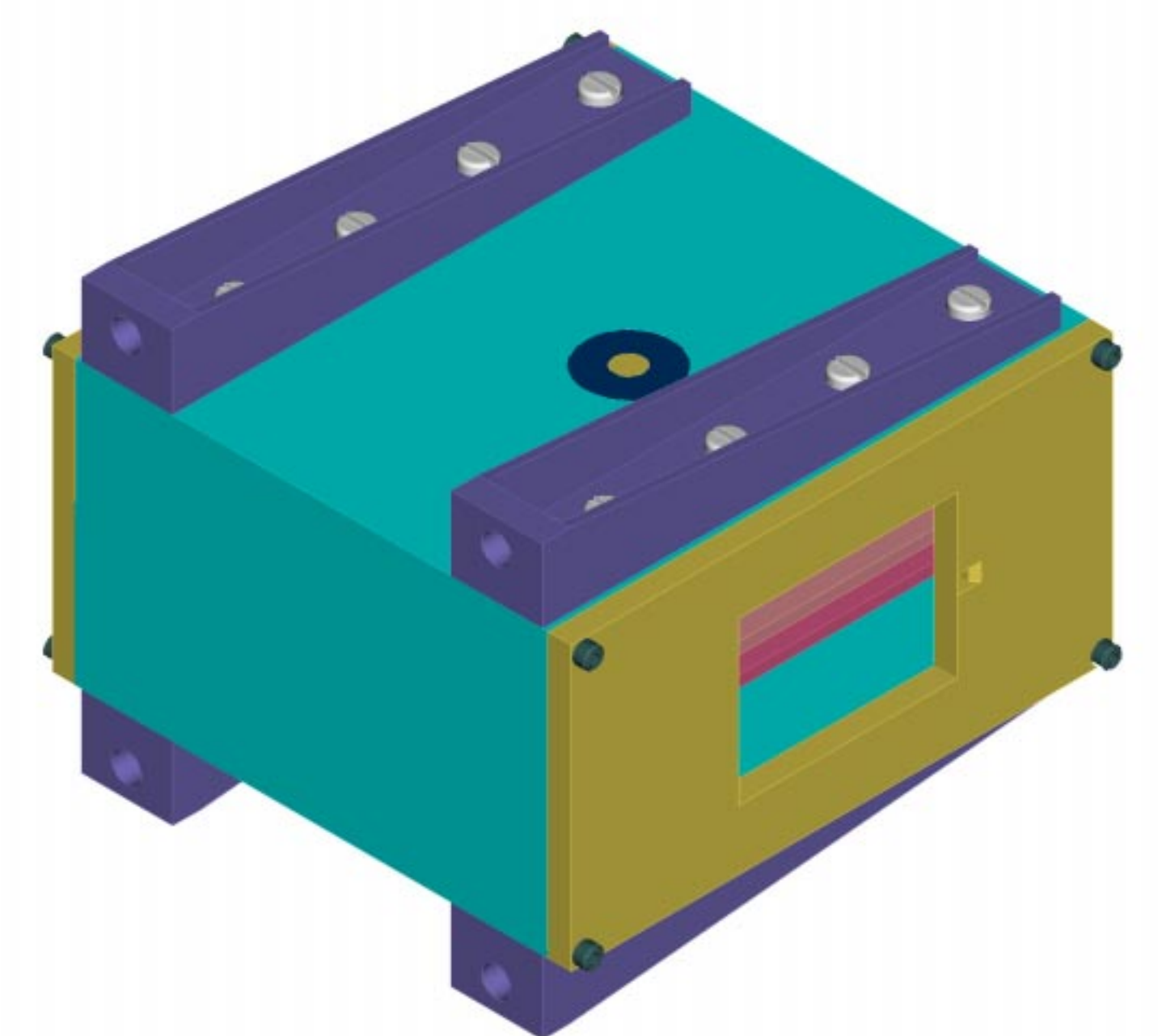

Figure 6.

The instrument pieces were mostly fabricated out of Carpenter Technology Corporation Electrical Iron with the exception of the legs, which were aluminum, the E-shaped pole separator clamps and alignment posts which were 70-30 cupro-nickel, two black delrin holders for the E-clamps, and, of course, the magnets themselves which were neodymium iron. All screws were 300 series stainless. Figure 7 shows some of the fabricated pieces.
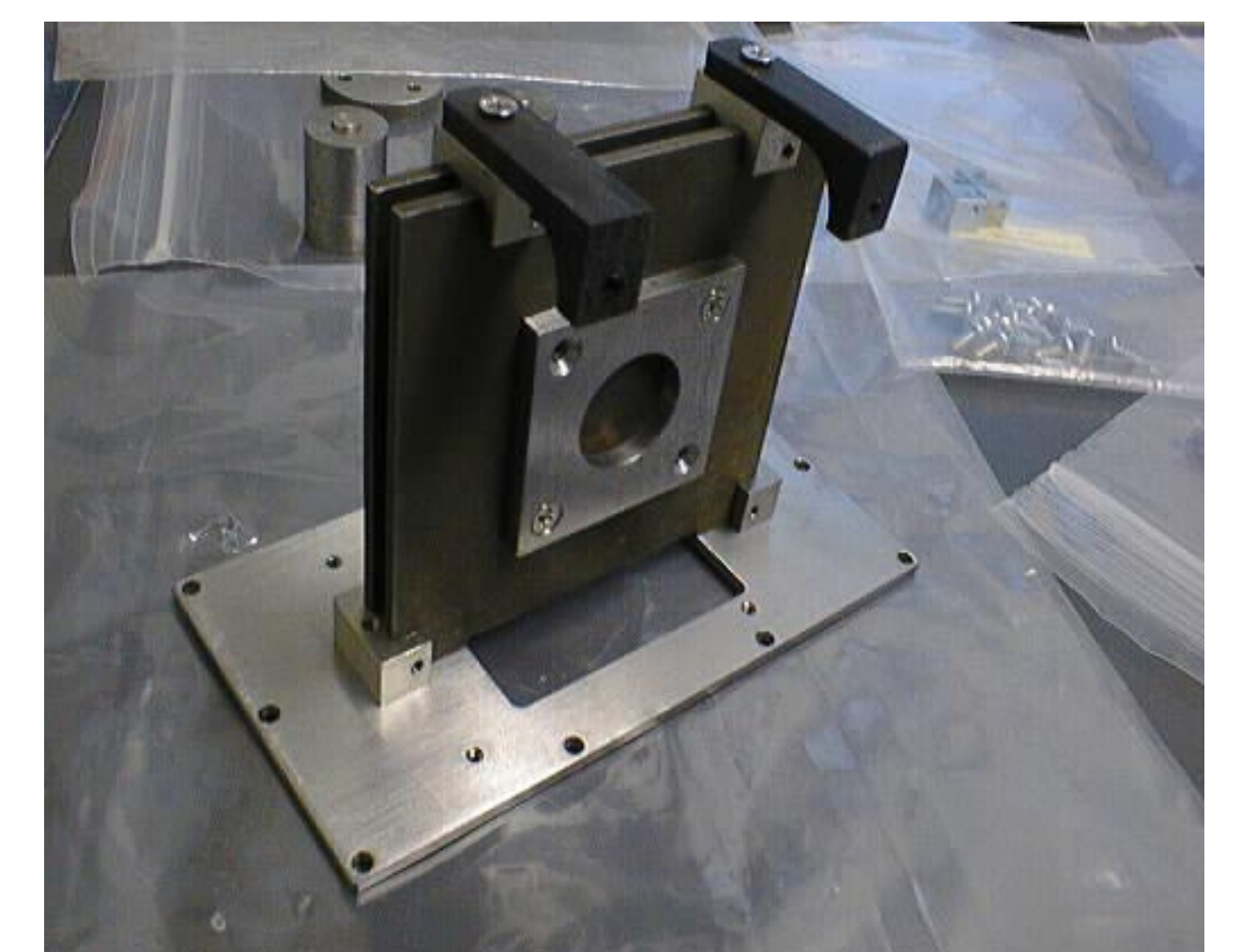

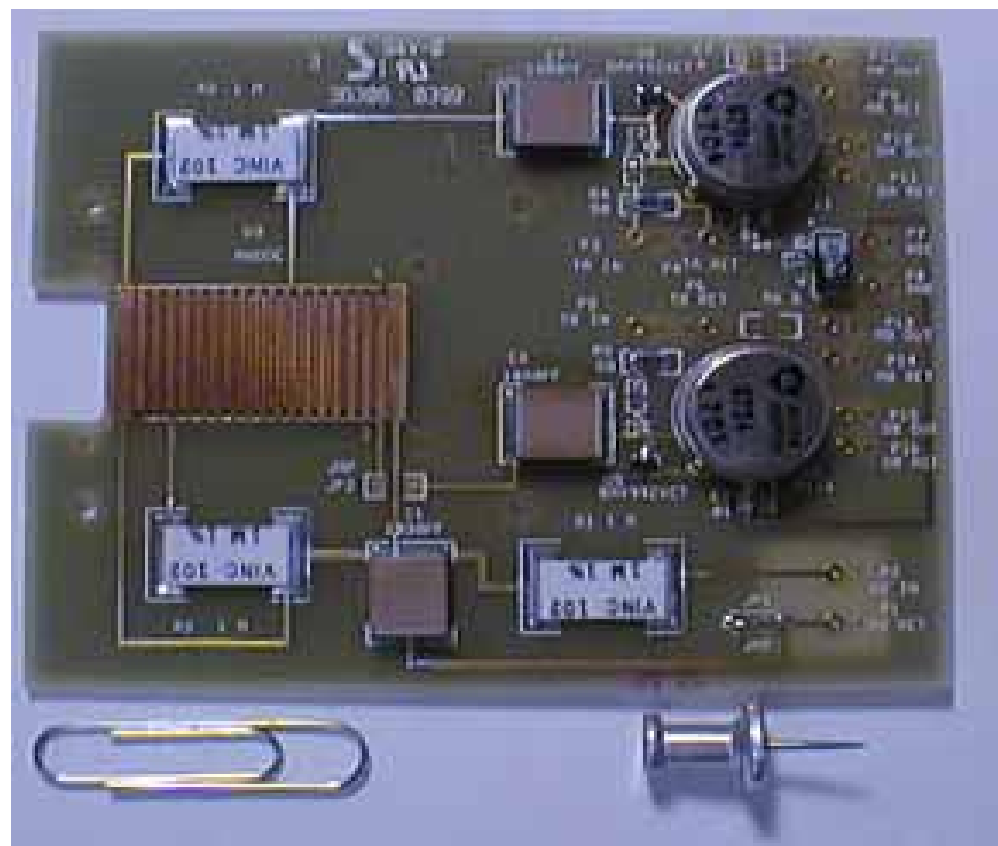Figure 7.

4. Position Sensing

Figure 8.

The position sensing was effected using a strip anode board (on the left of the board in Figure 8 to the right of the aperture indentation). There is nominally 5 mil spacing between the comb traces (4.1-5.5) with channel A varying from about 43 mil to about 11 mil in 2 mil increments with channel B varying from about 9 to about 41 mil in 2 mil increments. Each period is about 60 mil and there are 17 periods total running the length of the anode.

The copper strip widths on the anode board were carefully measured and logged. Figure 9 below shows a view of the traces from the anode board taken through a microscope. The black spaces are the five mil spacing between the traces.
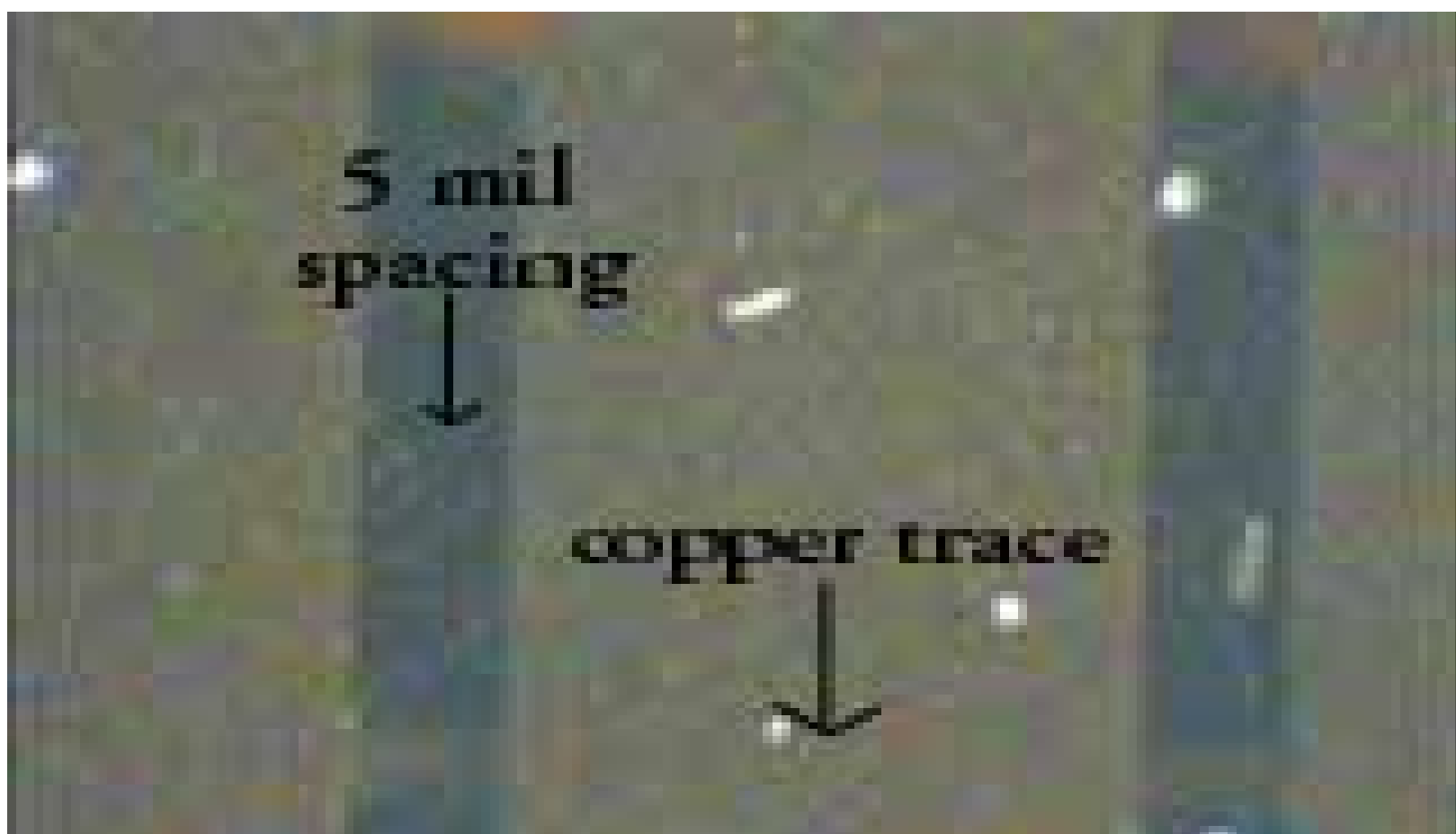

Figure 9.

Testing revealed that this anode configuration worked very well. Figure 10 shows the results of depositing charge on one side of the naked anode (in the assembled instrument, charge is deposited by the microchannel plates which multiply electrons). As expected, the output from the A channel is significantly higher than the B channel. The ratio is reversed on the other end of the anode board.
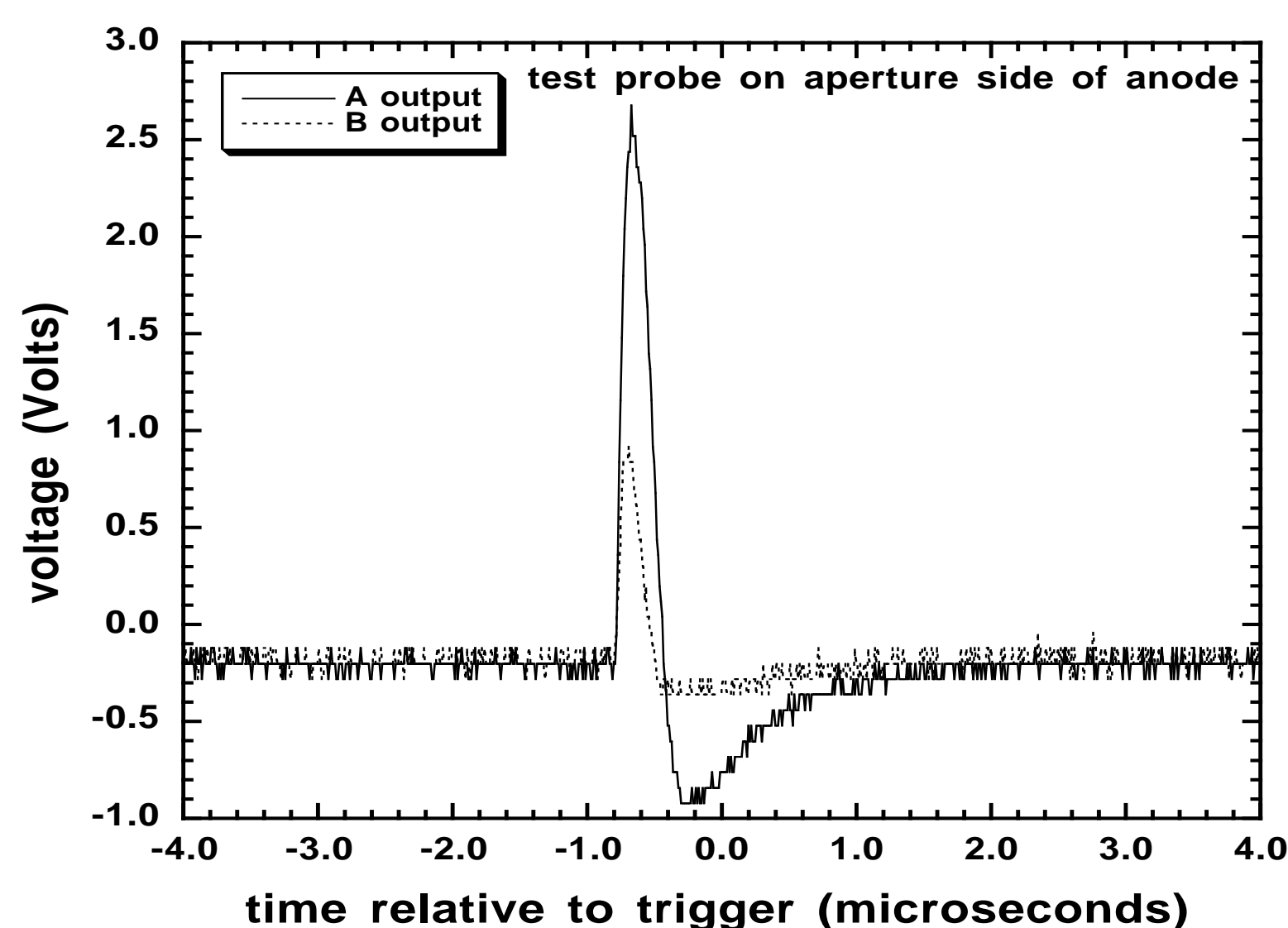

Figure 10.

The microchannel plate holder was constructed out of black delrin and was based, with slight modifications, on the design used for the Low Energy Neutral Atom (LENA) imager start assembly, shown below in Figure 11.

The black delrin is a dielectric. To avoid potential problems associated with the delrin charging up, the exposed portions of the holder were plated with platinum, as shown in the figure below, Figure 12.
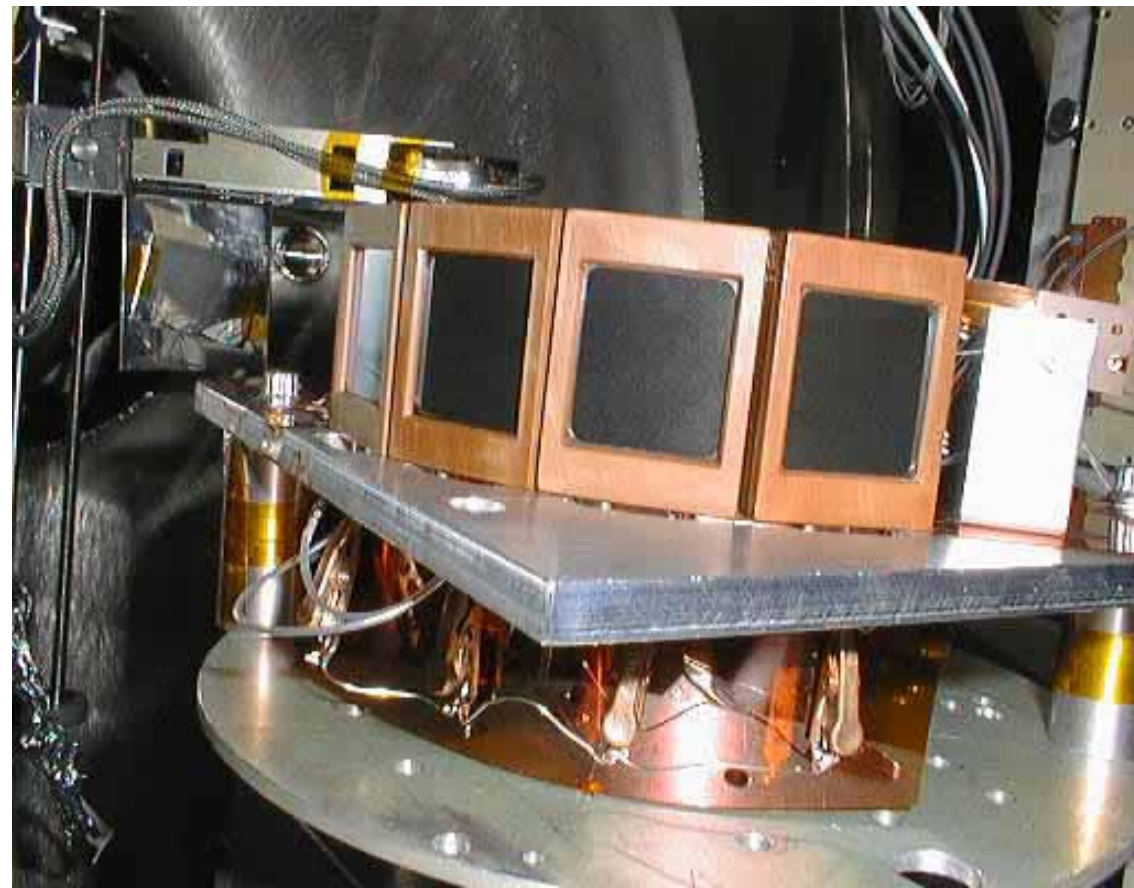

Figure 11.

Figure 12.

The microchannel plate holder itself (1 in Figure 13) holds a stack that includes (2) a grounded 100 lpi mesh to assure that electric fields associated with the microchannelplate assembly do not creep into the field region and affect the electron trajectories, (3) a Rigiflex contact, borrowed from LENA, to establish ground on the mesh, (4) a 3.5 mil molybdenum spacer, (5) a Rigiflex contact to establish the potential on the top microchannel plate (6). The two 60 mil microchannel plates (borrowed from LENA) are separated by a 3.5 mil molybdenum spacer (6,7 and 8). We opted not to use an intermediate voltage on the channel plates because these plates were already matched. Another Rigflex contact (9) established the voltage on the back of the microchannel plate stack. Finally, a 73 mil delrin spacer separated the stack from the anode board (10).
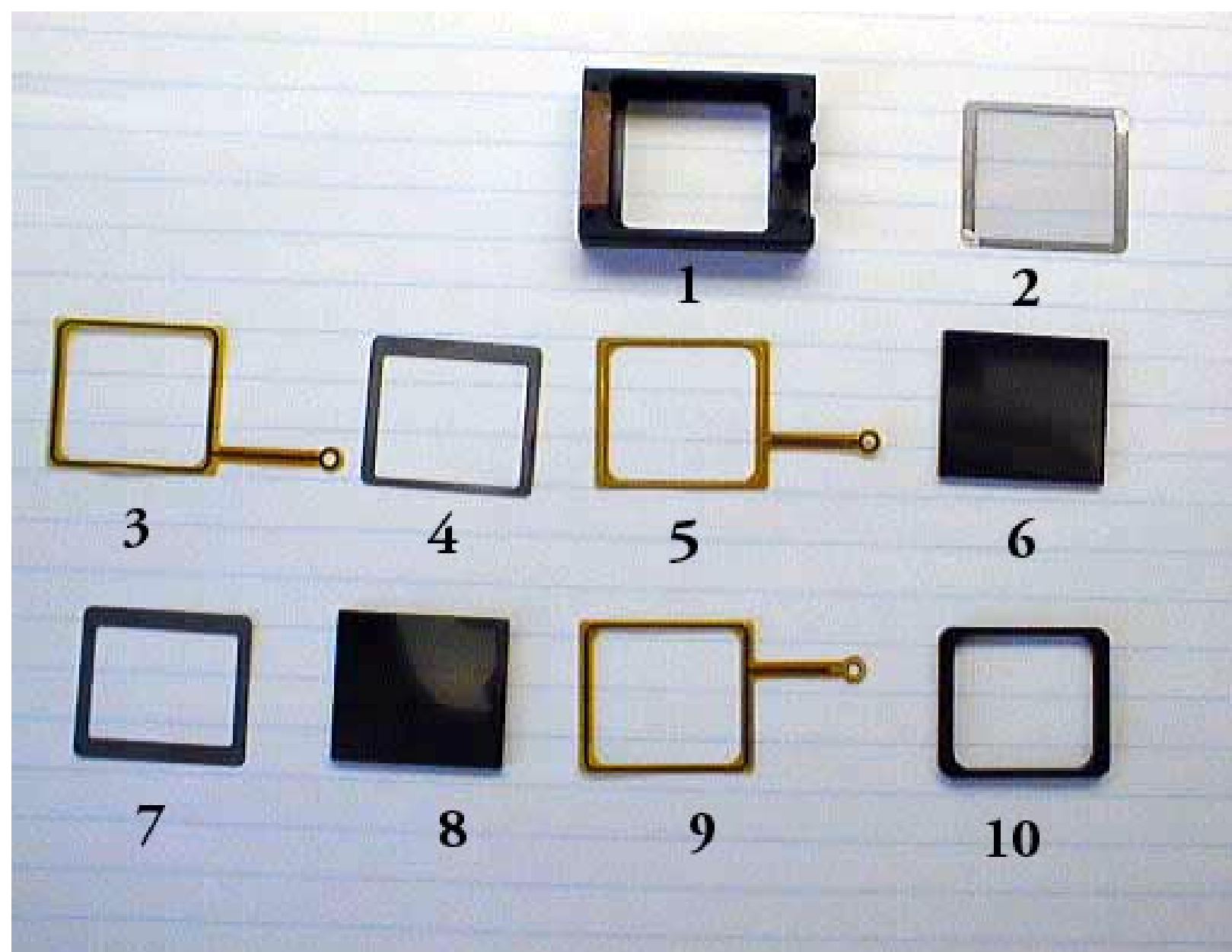

Figure 13.

The anode board, as illustrated by Figure 14 attaches to the front plate using 3 millimeter standoffs. The microchannel plate holder protrudes into the housing through the large rectangular opening to the left of the 2 millimeter by 3 millimeter entrance aperture.

Figure 14.

5. Mechanical Assembly

The Dexter Corporation Magnetic Technologies neodymium iron segments shown on the right hand side below (Figure 15 -- 30, 60 and 180 degree segments) were designed to fit between the inner and outer flux tubes in the drawing on the left below. The magnet segments are represented in orange.

In the final version of the insrument, the maximum field obtained using four 180 degree wedges was 280 gauss. The instrument was tested, however, using four 60 degree wedges which produced a field of 98 gauss because this field strength was more convenient for the range of electron energies our gun and its set-up could produce.
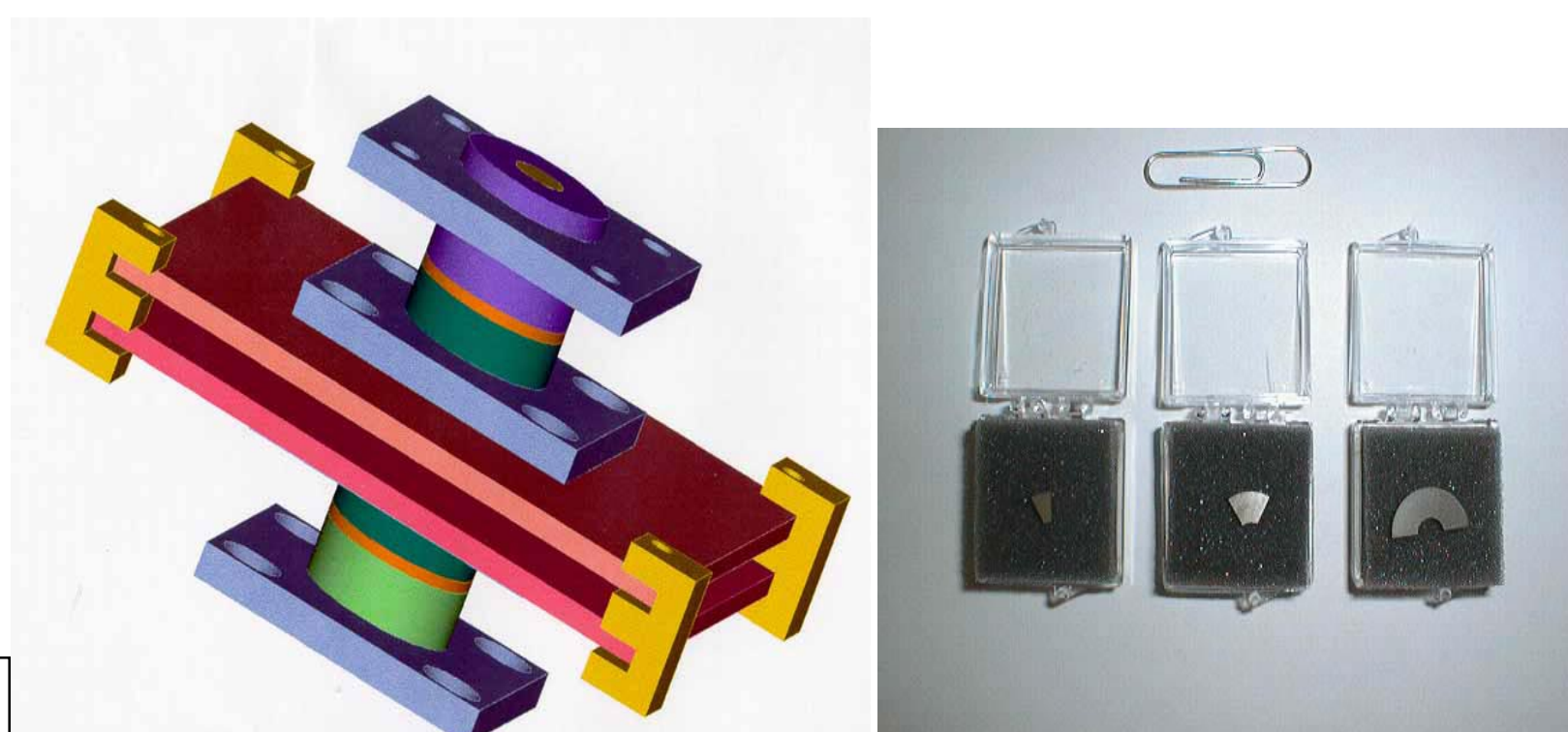

Figure 15.

One interesting aspect of this instrument noticed during the trajectory simulations and illustrated in Figure 16, is that the electrons tend to focus in realistic field geometries slightly before the detector plane. The distance before depends on the field gradient near the edge of the pole faces. Insofar as about half the gradient may be considered a field-free region, this scale length for focussing is expected.
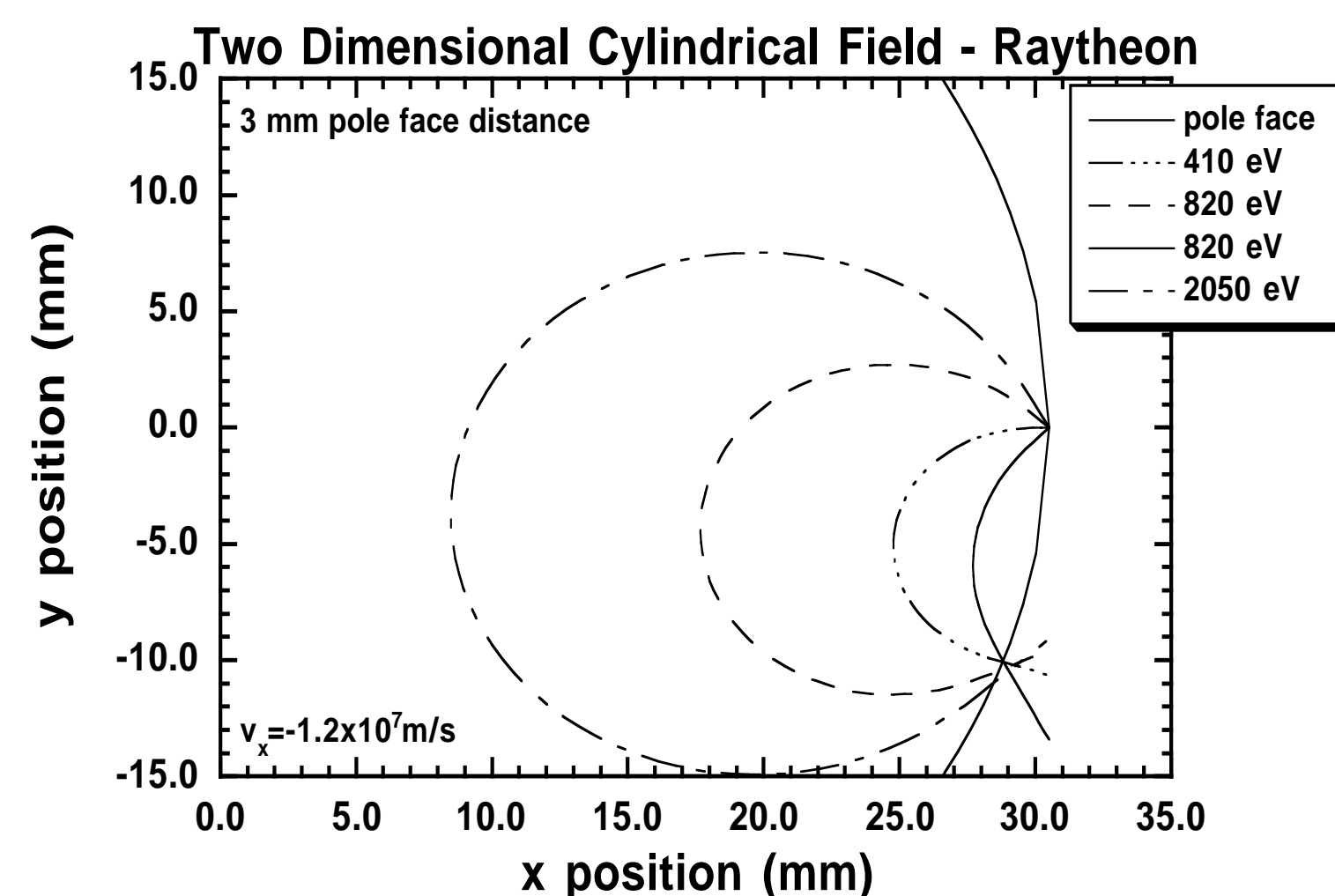

Figure 16.

To mitigate this effect, the microchannel plate assembly was designed to protrude into the field, as shown in Figure 17 below. The microchannel plate assembly is attached to the anode board at the bottom which is, in turn, attached to the electrical iron front plate. The pole faces, one of which is shown in the figure standing vertical, have a one millimeter notch in them to allow the front of the channel plates to sit close to the actual focussing position.
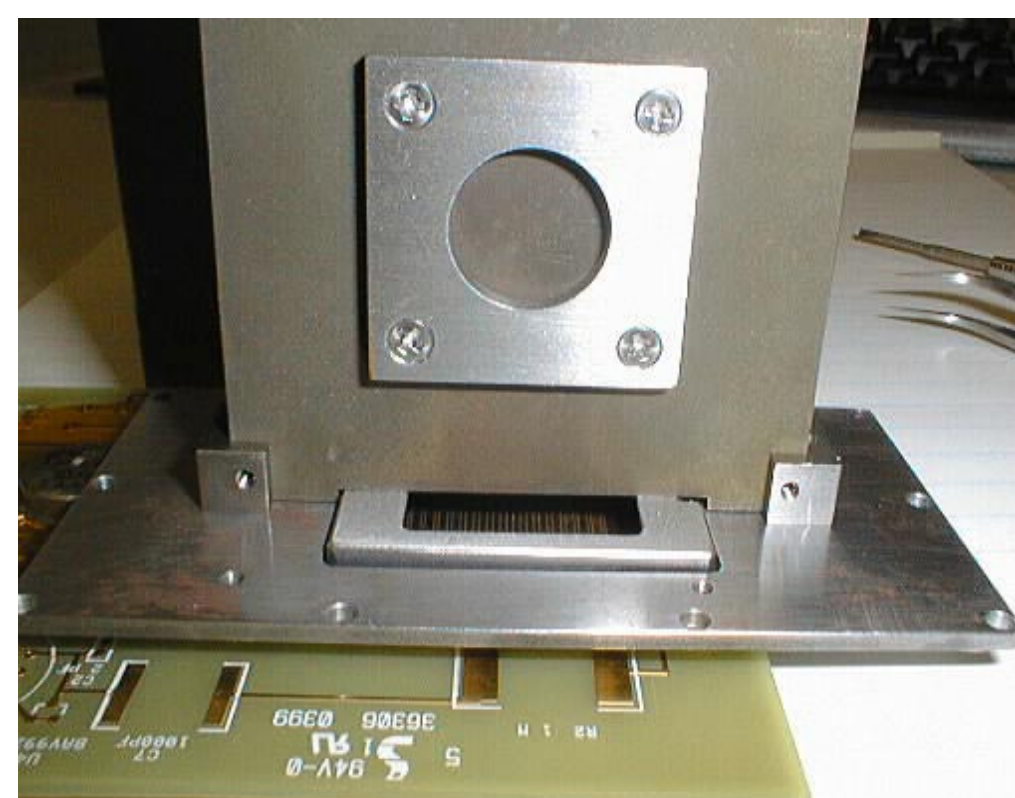

Figure 17.
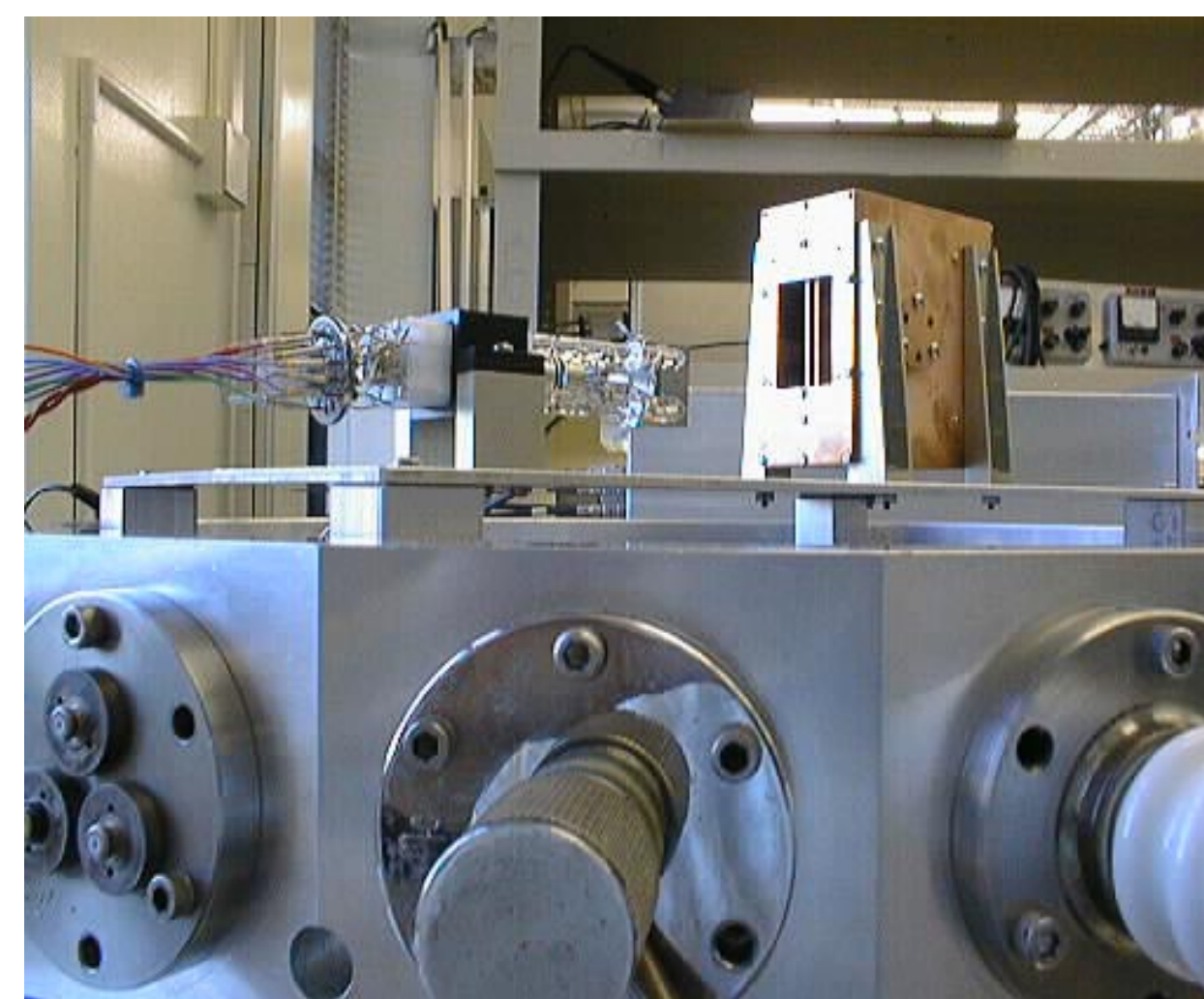
6. Preliminary Test Results

Figure 18.

Initial testing was performed by setting the instrument up arranged for normal incidence in front of the electron gun. Figure 18 above shows the instrument in the chamber without the front plate on it.
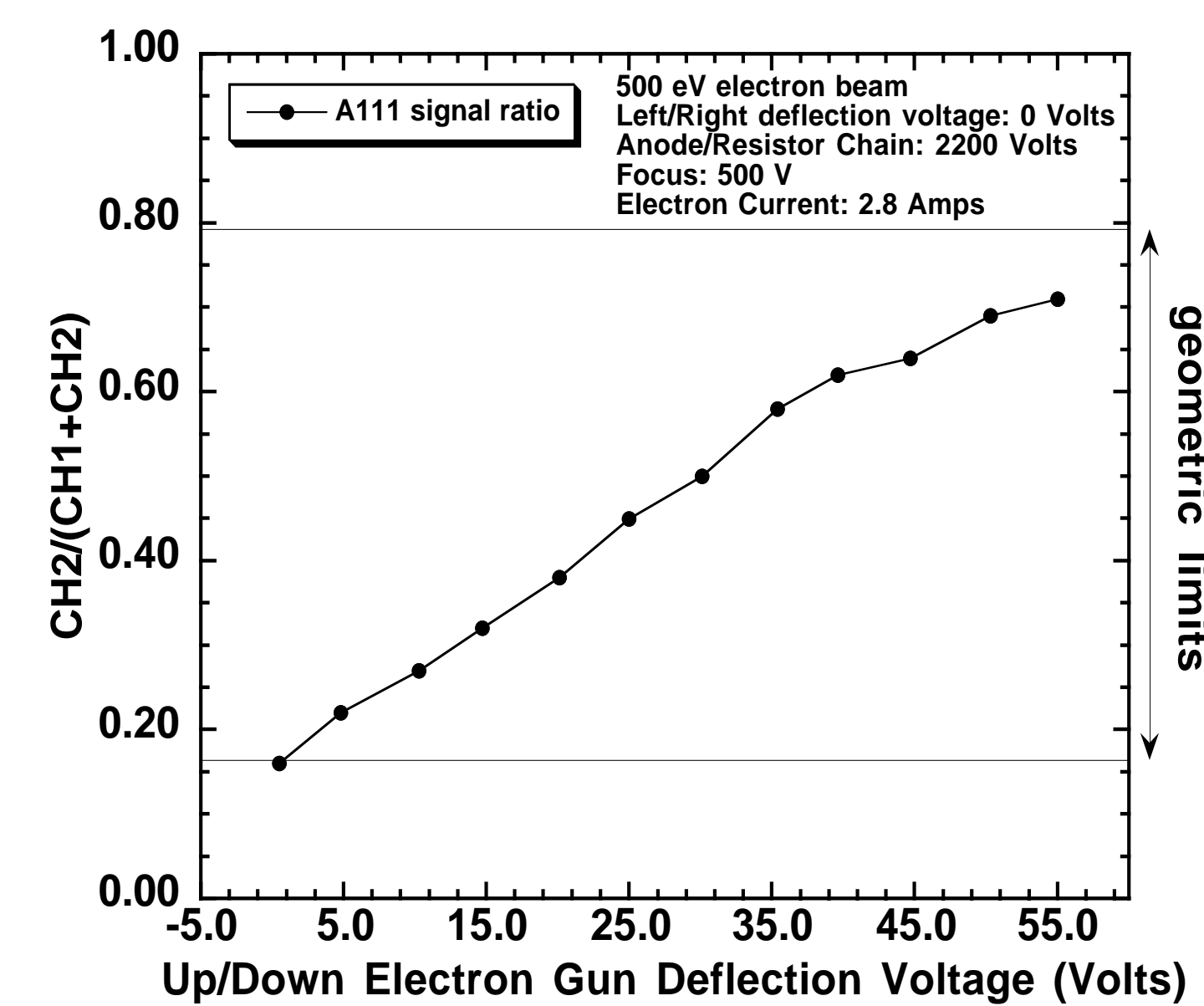

Figure 19.

One of the first test performed was a validation of the position sensing using an actual electron beam. Figure 19 shows the results of firing an electron beam directly into the channel plate assembly and varying the up/down deflection voltage on the gun. The position sensing is reasonably linear over the range between the expected geometric limits determined by the final ratios of the strip anode.
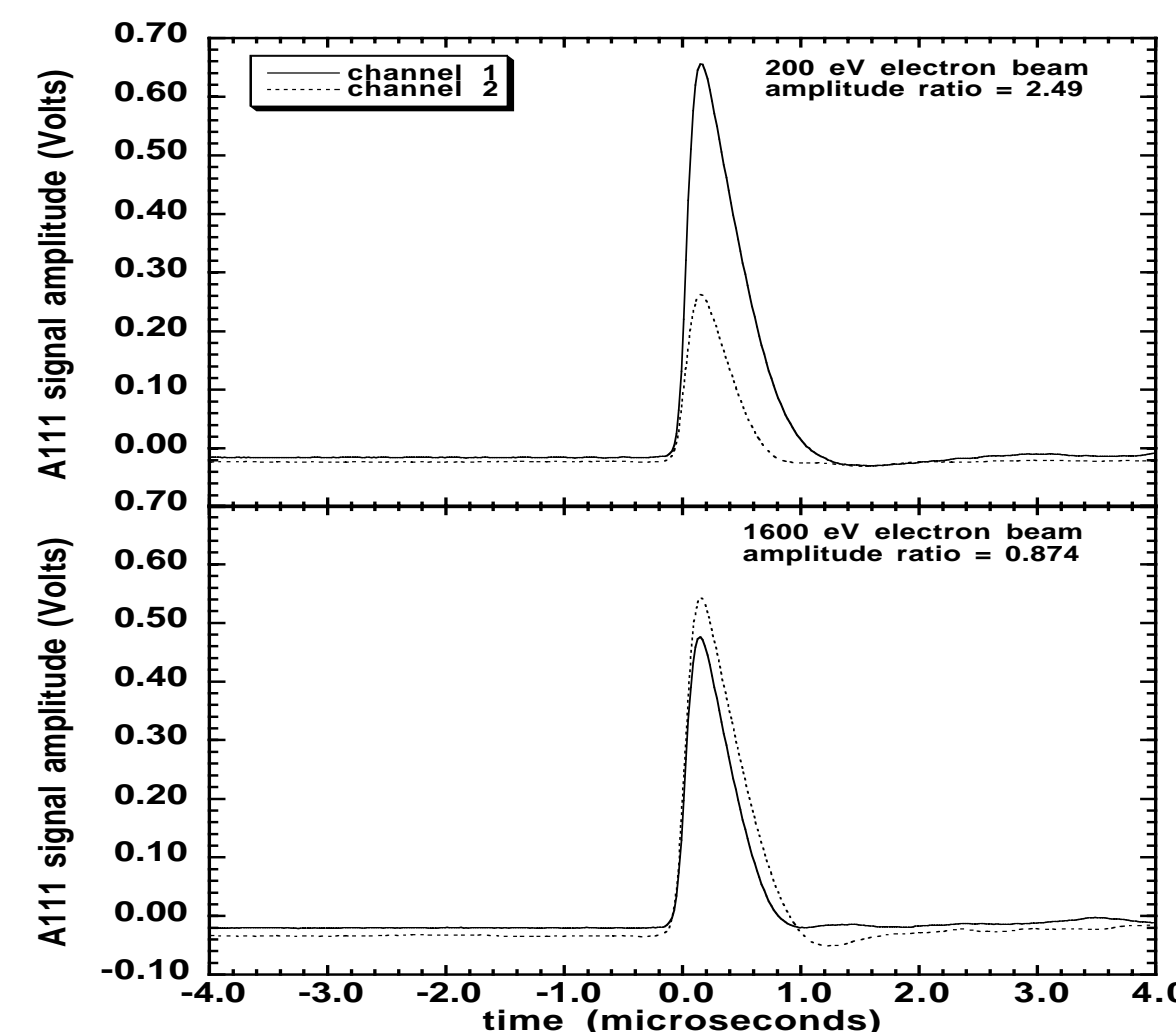

Figure 20.

Figure 20 shows the A111 output signals for electron beams entering the instrument at normal incidence with energies of 200 eV (top panel) and 1600 eV (lower panel). The ratios of the two signals is significantly higher for the lower energy beam which hits closer to the aperture.